Physicochem. Probl. Miner. Process., 58(5), 2022, 150265

http://www.journalssystem.com/ppmp

Physicochemical Problems of Mineral Processing

ISSN 1643-1049

Comparison of sorption capacity of biochar-based sorbents for capturing heavy-metallic ions from water media

Justyna Bąk

Department of Inorganic Chemistry, Institute of Chemical Sciences, Faculty of Chemistry, Maria Curie-Skłodowska University, Maria Curie-Skłodowska Sq. 2, 20-031, Lublin, Poland

Corresponding author: justyna.bak@mail.umcs.pl

Abstract: To develop the sorption efficiency of heavy metals: Cd(II), Co(II), Zn(II) and Pb(II) ions the biochar was modified by chitosan, $FeSO_4$ and $NaBH_4$. The morphology, physical structure and chemical composition of the biochar based sorbents were characterized by the scanning electron miscroscopy method, N_2 adsorption and desorption isotherms, X-ray diffractometry as well as the Fourier transform infrared spectroscopywith the attenuated total reflectance analyses. The research of M(II) ions sorption was carried out as a function of pH (2-6), interaction time (0-360 minutes) and temperature (293, 313, 333 K). The maximum sorption was obtained by the ChBC for Zn(II) ions - 19.23 mg/g and for MBC-Pb(II) - 19.11 mg/g. Different kinetic models as well as both isotherm and thermodynamic equations were used the sorption data modelling. For Cd(II), Co(II) and Zn(II) ions the nonlinear regression of the Elovich equation gave the best fit for the experimental data. On the other hand, for Pb(II) ions, the nonlinear forms of pseudo first order and pseudo second order show a better match. The value of the correlation coefficient >0.960 determined from the Freundlich isotherm model is the highest suggesting a good fit to the experimental data. The thermodynamic parameters: $\Delta G°$, $\Delta H°$ and $\Delta S°$ were listed and indicated that the process is spontaneous and endothermic in nature. The desorption efficiency was determined with the use of nitric, hydrochloric and sulfuric acids and the largest desorption yield for Pb(II)-ChBC equal 99.5 % was gained applying HNO_3.

Keywords: biochar, chitosan, magnetic, M(II) ions sorption, nonlinear regression

1. Introduction

One of the available and cheap sorbents that has been gaining popularity recently is biochar which is a product of biomass heating (Dai et al., 2021). Biochar can be defined as a porous, fine-grained char, characterized by a large content of organic carbon and small susceptibility to degradation. Both the elemental composition and the structure of biochar are related to the origin of raw materials and the heating conditions (Tan et al., 2017). Unlike carbon found in most organic matter the heating process changes the chemical environment of carbon which is conducive to the formation of aromatic structures (Qambrani et al., 2017), (Qu et al., 2020). Biochar is composed of stable or solid carbon, labile carbon, volatile compounds, moisture and ash. The other parameters affecting the sorption properties are the specific surface area, porosity, pH of biochar, ash content, surface charge, functional group content, volatile matter content, carbon, hydrogen, oxygen and other compounds, including minerals (Amalina et al., 2022). By the appropriate selection of the conversion process conditions, such as temperature, heating and retention time, it is possible to obtain biochars with appropriate physicochemical properties (Rajapaksha et al., 2016), (Rangabhashiyam et al., 2022). In many cases, it turns out that the properties of pristine biochar are not satisfactory. In other papers, the authors activate the surfaces of biochar by the use of acids, bases or various oxidizing agents, such as H_2O_2 and $KMnO_4$ (Lee & Shin, 2021), (Farhangi-Abriz & Ghassemi-Golezani, 2021) or modify biochars applying alginates, hydrogels, chitosans or magnetic particles: Fe, Fe_3O_4 (Li et al., 2021), (Xie et al., 2021) and others. Modification or activation applying various compounds results probably in changes of morphological, physical and chemical properties of biochar.

DOI: 10.37190/ppmp/150265

Chitosan is an inexpensive, renewable biopolymer found in large amounts in nature. Chitosan powders, flakes or beads function very well as alternative sorbents (Eltaweil et al., 2021). It is also used as a biochar surface modifying agent. The advantage of the biochar and chitosan the combination is a relatively large surface area of biochar with the great chemical affinity for chitosan. This proves that the chitosan modified biochars bind effectively heavy metal ions from aqueous media (Zhou et al., 2013). Tan et al. (Tan et al., 2022) synthesized a novel chitosan modified kiwi branch biochar and applied this sorbent to remove Cd(II) ions from wastewater. The results showed better capture od Cd(II) ions with the sorption capacity equal 118.43 mg/g.

Magnetically modified biochar (MBC) has been successfully used for water and wastewater treatment and recovery of heavy metals. The advantage of using MBC is the possibility of separating heavy metals from aqueous solutions after the adsorption process by means of a magnetic field. In the research carried out by Gong et al. (Gong et al., 2020) magnetic biochar was obtained from the pyrolysis of wheat straw at 573 K and 973 K and synthesized using the Fe^{2+}/Fe^{3+} solution ($FeCl_3 \cdot 6H_2O$ and $FeCl_2 \cdot 4H_2O$) and precipitated by means of NaOH solution. The results of the test proved that MBC could efficiently remove lead (25.1-42.1%) from polluted soils. Additionally, Pb(II) ions can be successfully removed from aqueous solutions using the zero valent iron magnetic biochar composites. For biochar magnetization $FeCl_3 \cdot 6H_2O$ was applied and the maximum sorption capacity was found to be 60.8 mg/g (Rama Chandraiah, 2016).

Modification of the biochar surface was made using (1) chitosan designated ChBC and (2) $FeSO_4$ and $NaBH_4$ designated MBC. Consequently, the aims of this paper were (-) to characterize the physicochemical features of ChBC, and MBC, (-) to compare key parameters affecting heavy metal ions (Cd(II), Co(II), Zn(II), Pb(II)) sorption on ChBC and MBC, (-) to determine a possible mechanism of the sorption process and (-) to propose a proper desorption process for regeneration of ChBC and MBC as well as metal recovery.

2. Materials and methods

2.1. Sorbents preparation and physical and chemical characterization

Earthcare (USA) produces biochar (BC) for the experiment by gasifying agricultural wastes. Sigma Aldrich (Poland) provided the chitosan for the experiment which was applied in the powder form without any prior processing. Chitosan modified biochar (ChBC) was obtained by dissolving 2 g of chitosan in 100 cm^3 of 2 % solution of acetic acid (analytical grade, Avator Performance Materials, Poland) while stirring for 24 hours with a magnetic stirrer at 1000 rpm at room temperature. Next 16 g of biochar was added to the mixture and stirred for 30 minutes. To precipitate the suspension, 100 cm^3 of a 3 % sodium hydroxide solution was added in the next step. It was then agitated for 2 hours before being rinsed with distilled water. When the mixture was neutral, it was filtered at a lower pressure. The resulting material (ChBC) was dried for 8 hours at 368 K in a laboratory oven before being ground.

Magnetic biochar was prepared by dissolving 4.96 g of $FeSO_4 \cdot 7H_2O$ (analytical grade, Acros Organics, Belgium) in 100 cm^3 distilled water in a beaker and mixing with 5 g of BC. Then 0.68 g of $NaBH_4$ (analytical grade, Sigma Aldrich, Poland) was added to the suspension while stirring at 1000 rpm for 360 minutes. Next the suspension was filtered and rinsed with distilled water before being baked in an oven at 368 K. The obtained material was designated MBC. Zerovalent iron is obtained according to the reactions:

$$4FeSO_4 + O_2 + 2H_2O \rightarrow 4Fe(OH)SO_4$$

$$4Fe^{3+} + 3BH_4^- + 12H_2O \rightarrow 4Fe^0 + 3H_2BO_4^- + 12H^+ + 9H_2$$

The effectiveness of biochars for the sorption of Cd(II), Co(II), Zn(II) and Pb(II) ions has been evaluated using a variety of analytical techniques. A scanning electron microscopy (SEM) examination was performed employing the Quanta 3D FEG (FEI, USA) equipment to evaluate the surface morphology of the biochar-based products. An ASAP 2420M sorption analyzer (Micrometrics, USA) was used to evaluate the low temperature N_2 adsorption/desorption isotherms and at 77 K. The BET specific surface area, pore diameter, total pore volume and micropore volume can be determined using this method. The degassing temperature was 473 K. To determine the crystalline phases contained in

the sorbents, X-ray diffraction (XRD) patterns of MBC and ChBC were recorded using a PANalytical X-ray diffractometer (Empyrean, Netherlands). The ATR technique was used to the study infrared spectra applying a Cary 630 FTIR analyzer (Agilent Technologies, USA). The FTIR technique provides a wavelength range of 4000-400 cm^{-1} and a spectral resolution of 4 cm^{-1} to make measurements of the functional groups present on the sorbents surface.

2.2. Methodology of pH and phase contact time investigations as well as kinetic and adsorption modelling

As a source of heavy metal ions $Cd(NO_3)_2{\cdot}4H_2O$, $Co(NO_3)_2{\cdot}6H_2O$, $Zn(NO_3)_2{\cdot}6H_2O$ and $Pb(NO_3)_2$ were applied. The reagents of analytical grade were dissolved in distilled water and contained 1000 mg/dm^3 of M(II) ions stock solutions. The solutions of HNO_3 (Chempur, Poland) and NaOH (Chempur, Poland) were added to obtain the proper pH. The chemicals were of the highest analytical quality. The research was carried out using a static technique. To evaluate the performance of the sorbents under different conditions, the effect of pH, interaction time, initial ions concentration and temperature was accomplished. The samples (0.1 g of sorbent and 20 cm^3 of solution) were placed in a mechanical shaker type 358 A (Elpin+, Poland) with the constant vibration amplitude (8 units) and their contents were mixed at pH 2, 3, 4, 5 and 6 at 100 mg/dm^3 of solutions with a 180 rpm shaking speed for 360 minutes at 295 K. After shaking the sorbent was separated from the aqueous media by filtration and the pH of the filtrate was measured applying the pHmeter pHM82 (Radiometer, Denmark). The concentration of the filtrate was measured by means of atomic absorption analyzer Spectr AA240 FS (Varian, USA) at 228.8 nm for Cd(II), 240.7 nm for Co(II), 213.9 nm for Zn(II) and 217.0 nm for Pb(II). The optimal solution pH was established. The estimation of pH value impact and the effect of interaction time (1-360 minutes) was made at 180 rpm and 293 K. The amounts of the adsorbed M(II) ions q_t (mg/g) and the sorption percentage (%S) were calculated applying the expressions presented in (D. Kołodyńska, Krukowska, et al., 2017). In order to calculate the theoretical sorption capacity, determination coefficient and Chi-square errors there were applied the nonlinear kinetic models: pseudo first order (PFO) (Eq.1), pseudo second order (PSO) (Eq.2), Elovich (Eq.3) expressed by the equations:

$$q_t = q_e(1 - exp(-k_1 t)) \tag{1}$$

$$q_t = \frac{k_2 {q_e}^2 t}{1 + k_2 q_e t} \tag{2}$$

$$q_t = \left(\frac{1}{\beta}\right) ln(1 + \alpha\beta t) \tag{3}$$

where: q_e (mg/g) is the amount of ions adsorbed per amount of sorbent at equilibrium, k_1 (1/min) and k_2 (g/mg·min) are the equilibrium rate constants of the PFO and PSO, respectively, α (mg/g·min) is the initial adsorption rate, β (g/mg) is the desorption constant which is related to the chemisorption activation energy and the surface coverage range. The Chi-square errors were calculated based on the Origin software according to the equation:

$$\chi^2 = \sum \frac{{(qe,cal}^2{}_{e,exp}}{q_{e,cal}} \tag{4}$$

where: $q_{e,exp}$ is the amount of M(II) ions adsorbed at equilibrium determined experimentally and $q_{e,cal}$ is the adsorption capacity determined from the kinetic model.

The equilibrium investigations were carried out using the following method: 0.1 g of sorbent and 20 cm^3 of solution with 50-600 mg/dm^3 concentrations. The adsorption parameters were calculated from the Langmuir (Eq.5), Freundlich (Eq.6) and Temkin (Eq.7) nonlinear isotherms presented by the equations:

$$q_e = \frac{q_0 K_L C_e}{1 + K_L C_e} \tag{5}$$

$$q_e = K_F C_e^{1/n} \tag{6}$$

$$q_e = B\, ln(AC_e) \tag{7}$$

where: q_0 (mg/g) is the monolayer sorption capacity, C_e is the equilibrium concentration (mg/dm^3), K_L (dm^3/mg) is the characteristic constant for the Langmuir equation, K_F (mg/g) is the adsorption capacity characteristic of the Freundlich model, 1/n is the Freundlich constant related to surface heterogeneity.

The value of 1/n>1 indicates the weak adsorptive bond between the adsorbate and adsorbent molecules, the value of 1/n<1 indicates the strong adsorptive bond due to strong intermolecular attractions in the adsorbent layers. Based on the Temkin model: A and B are Temkin isotherm constants related to the heat of adsorption.

In order to calculate the thermodynamic parameters and to investigate the nature of the sorption process of M(II) ions, the influence of temperature change on the efficiency of metal ions removal was studied. The investigations were carried out at 293, 313 and 333 K for the same solutions concentrations as those in the adsorption studies. The parameters: changes in the standard free energy (ΔG°), standard enthalpy (ΔH°) and standard entropy (ΔS°) were calculated using the equations:

$$\Delta G^0 = -RT\, ln\, K_d \tag{8}$$

$$\Delta G^0 = \Delta H^0 - T\Delta S^0 \tag{9}$$

$$K_d = \frac{C_s}{C_e} \tag{10}$$

$$ln\, K_d = \frac{\Delta H^0}{RT} + \frac{\Delta S^0}{R} \tag{11}$$

where: R is the gas constant (J/mol·K), T is the temperature (K), K_d is the distribution coefficient, C_s and C_e (mg/dm^3) are the sorption capabilities of the adsorbent and adsorbate phases, respectively (D. Kołodyńska, Bąk, et al., 2017).

The activation energy (E_a) of M(II) ions adsorption on the ChBC and MBC can be calculated by Arrhenius expression:

$$ln\, k_2 = ln\, k_0 - \frac{E_a}{RT} \tag{12}$$

From the dependence ln k_2 versus 1/T, E_a can be calculated from the slope.

2.3. Reusability of MBC and ChBC

In order to evaluate the reusability of MBC and ChBC, the impact of the kind of desorbing agent was assessed, taking into consideration the reuse of these sorbents. Furthermore, the reversibility of the Cd(II), Co(II), Zn(II) and Pb(II) ions sorption on the sorbents offers essential information on the process mechanism. The dried and weighed sorbents after the sorption (starting solution concentration 100 mg/dm^3, time 360 minutes, pH 5, shaking speed 180 rpm and temperature 293 K) were shaken with the nitric, hydrochloric and sulfuric acids (analytical grade, Avator Performance Materials, Poland) for 360 minutes. The desorption yield was calculated applying the expression:

$$\%desorption = \frac{C_{des}}{C_0 - C_t} 100\% \tag{13}$$

where: C_{des} (mg/dm^3) is the concentration of ions after the desorption.

3. Results and discussion

3.1. Morphological and physical properties

The ChBC and MBC composites of the micrographs present the surfaces morphologies indicating that two sorbents are characterized by the irregular surface texture (Fig. 1).

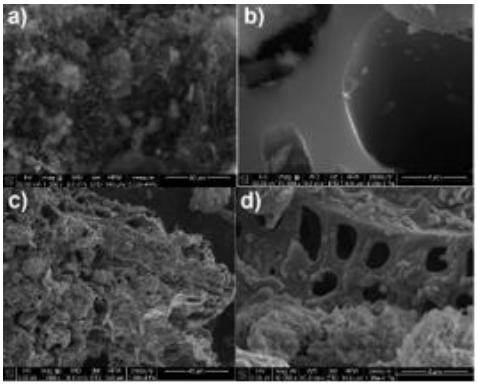

Fig. 1. SEM images of (a,b) ChBC, (c,d) MBC at 1000x (a,c) and 10000x (b,d) magnifications

The physical properties of the ChBC and MBC varied depending on the modification technique. ChBC exhibited the smallest surface area equal 128 m^2/g compared to that of MBC equal 158 m^2/g. These values are larger than the BC surface area equal 116 m^2/g (Kołodyńska, Krukowska, et al., 2017). The total pore sizes are 6.2 and 8.2 nm for ChBC and MBC, respectively. The total pore volume and micropore volume are 0.093 and 0.039 cm^3/g for ChBC as well as 0.160 and 0.038 cm^3/g for MBC. MBC has the large specific surface area compared to that of ChBC hence it is to be expected that MBC will have a greater ability to remove heavy metal ions due to the increased number of adsorption centres. The isotherms shape (Fig. 2) resembles type IV according to the IUPAC classification. This type is characteristic of the micro- and mesoporous adsorbents. At smaller relative pressures, the micropores are filled first and the increase in the pressure leads to the formation of a monolayer. As the pressure increases, multilayer is formed. Additionally, the pore size distribution from the N_2 adsorption isotherm curves confirms domination of mesopores (2-50 nm) in the sorbents structure (Sbizzaro et al., 2021).

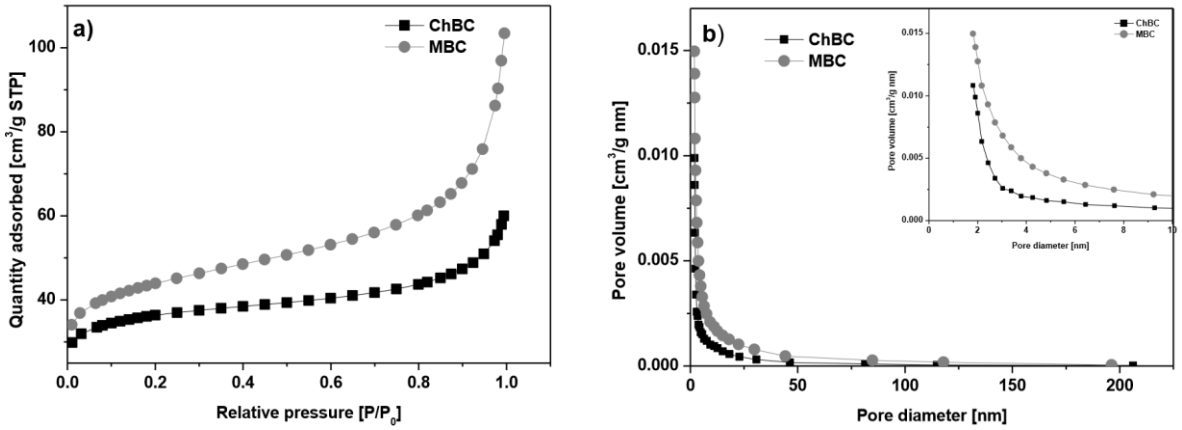

Fig. 2. (a) N_2 adsorption/desorption isotherms of ChBC and MBC, (b) pore size distribution of ChBC and MBC

3.2. Chemical properties

The XRD diffractograms (Fig. 3) show that silica is the crystalline phase with the largest content and the intensity at approx. 2Θ = 20.85 and 26.47. The peaks at approx. 2Θ = 29.43 and 30.92 are related to the presence of carbon in the sorbents: $CaCO_3$ and $CaMgCO_3$, respectively (Han et al., 2015). For the MBC appearance of the peak at approx. 44.65 is related to Fe confirming the modifications effectiveness (C. Wang & Wang, 2018). The SiO_2 peak of chitosan modified biochar has a greater intensity than that of magnetic biochar. The other less intense crystalline phases present in the materials include: $Na(AlSi_3O_8)$, $K(AlSi_3O_8)$ and $CaCl_2$.

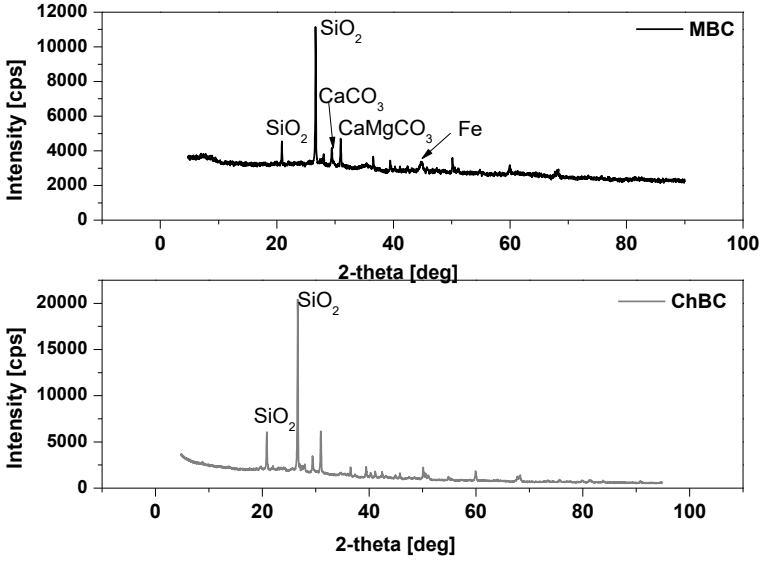

Fig. 3. XRD patterns for ChBC and MBC

The ATR-FTIR spectra of ChBC and MBC are presented in Fig. 4. The stretching vibration of -OH in phenols and alcohols are responsible for the peaks in the range of 3847-3662 as well as 3544 and 3445 cm^{-1} originating from O–H stretching vibrations of H-bound hydroxyl groups (Dudek & Kołodyńska, 2022), (Janu et al., 2021). The weak peaks at 3391, 3364, 3290 and 3192 cm^{-1} correspond to the stretching vibrations of -NH. The acetylene polymerization was indicated by the peaks due to the saturated C-H stretching vibrations the ChBC surface at approximately 2894 cm^{-1} (Zhang et al., 2020), (Bozecka et al., 2016). The peaks in the range of 2000-2500 cm^{-1} are related to the presence of C≡C and C≡N bonds or cumulative C=C=C and N=C=O double bonds. The stretching vibrations of -CH_2 groups in the long aliphatic chains are related to the peaks at around 2000 cm^{-1} (Cui et al., 2016). The main absorption peaks were found in the sorbents at 1623 and 1563 cm^{-1} as well as 1408 and 1406 cm^{-1} originating from the stretching vibrations of asymmetric COO^- groups and those of symmetric carboxylate groups, respectively (Bai et al., 2020). Additionally, there are bands at 1016 cm^{-1} which are attributed to the vibrations of the C-O-C groups (Janu et al., 2021). The peaks in the range of 985-797 cm^{-1} indicate the presence of bending vibrations outside the plane of the C-H bond in the aromatic ring (Bai et al., 2020). The vibrations related to the binding of oxygen functional groups with iron occur at approx. 690 cm^{-1}. The shift of the bands of hydroxyl and carboxylate groups after the sorption process proves the binding of heavy metal ions by these groups.

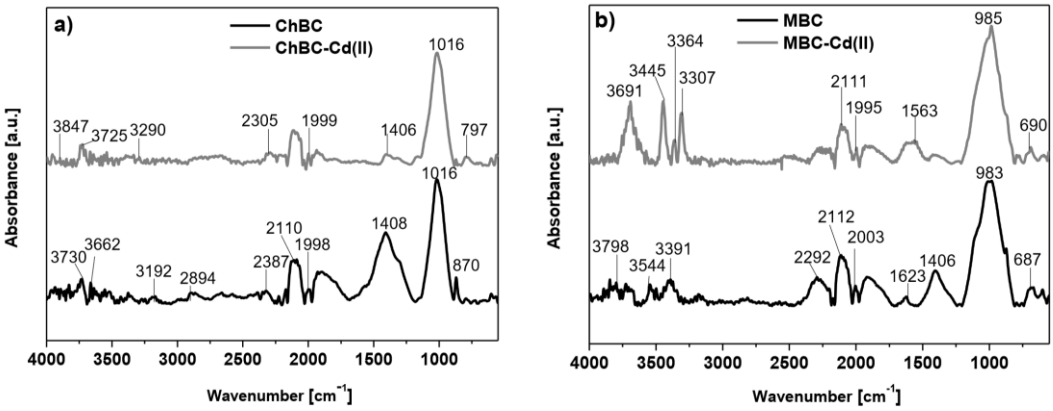

Fig. 4. ATR-FTIR spectroscopy of (a) ChBC and (b) MBC before and after the Cd(II) ions adsorption

3.3. Impact of pH

Fig. 5 illustrates the influence of pH in the range of 2-6 on the sorption process of M(II) ions on ChBC and MBC. This pH range was chosen because, according to the speciation diagrams presented in the papers (Kołodyńska, Bąk, et al., 2017), (Sharaf El-Deen et al., 2017), (Sočo & Kalembkiewicz, 2015), (Huang et al., 2017) up to pH 8, the doping form of Cd(II), Co(II), Zn(II) and Pb(II) ions is the form M^{2+} (see in the Supplementary Materials - Fig. S1, S2). The q_t values for all ions increase with the increasing pH to the value 5 and at pH 6 decrease because above 6 the metal ions begin to precipitate in the hydroxide forms (Otrembska & Gega, 2013). At pH 5 the amounts of the adsorbed ions are: 16.99, 11.97, 18.83 and 16.98 mg/g for Cd(II), Co(II), Zn(II) and Pb(II) ions on ChBC and 15.67, 13.94, 15.46 and 18.62 mg/g for the above mentioned ions on MBC, respectively. The sorption percentage is the highest for the Pb(II) ions and equal to 99.8 and 99.9 % for ChBC and MBC, respectively (the sorption percentages are given in Fig. 5 was showed). The removal of Co(II) ions from the aqueous media proceeds with the smallest efficiency. For the solution of metal ions with the pH value of 2, the sorbents were characterized by the smallest adsorption capacity. As they are so closely connected with the hydronium ions, more accessible protons compete with the existing cations for the sorbent active sites at lower pH values. As the pH value rises, the concentration of hydronium ions drops. As a result, the negatively charged surface of the sorbent becomes more sensitive to the cation assault, increasing the sorbent sorption capacity (Aksu & Isoglu, 2005).

3.4. Impact of phase contact time

The obtained results in Fig. 6 confirm that the effectiveness of the sorption process of heavy metal ions

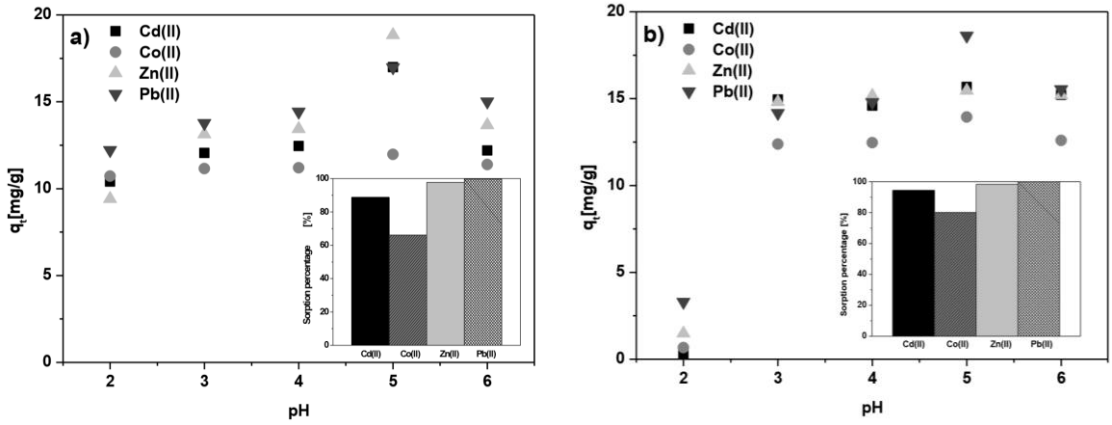

Fig. 5. Impact of pH on the sorption of Cd(II), Co(II), Zn(II) and Pb(II) ions on (a) ChBC and (b) MBC (C_0 100 mg/dm^3, t 360 min., shaking speed 180 rpm, temperature 293 K).

on the ChBC and MBC depends on the interaction time and rises with its increase. The amounts of the adsorbed ions after 360 minutes are: 17.59, 11.83, 19.23 and 17.41 mg/g for Cd(II), Co(II), Zn(II) and Pb(II) ions on ChBC as well as 15.82, 14.60, 15.49 and 19.11 mg/g for these ions on MBC, respectively. The sorption percentages for ChBC are: 70.1, 62.4, 94.1 and 99.8 % for Cd(II), Co(II), Zn(II) and Pb(II) ions and for MBC 92.5, 75.5, 96.5 and 99.9 % (pH 5, shaking speed 180 rpm, temperature 293 K). Co(II) ions attained the smallest q_t values for both sorbents. The shape of the curves indicates a two-step sorption process. In the first step, the process of ions absorbed from the solution takes up about 60 minutes because the amount of accessible centers is very large and the process is fast. In the second step it is slow lasting from 60 to 360 minutes because there are fewer free adsorption centers. The equilibrium state is established in the second stage. The accessibility of free ion centers on the sorbent surface justifies the two-step sorption process. According to the findings, 360 minutes is enough time for the adsorption isotherm equilibrium experiments.

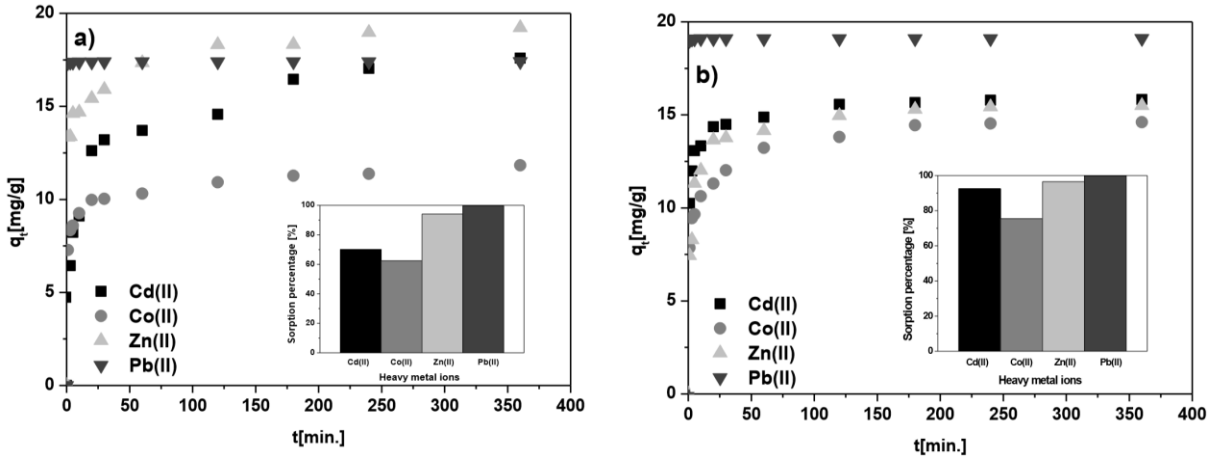

Fig. 6. Impact of interaction time on the sorption of Cd(II), Co(II), Zn(II) and Pb(II) ions on (a) ChBC and (b) MBC (C_0 100 mg/dm^3, pH 5, shaking speed 180 rpm, temperature 293 K).

3.5. Adsorption kinetics

The likely sorption mechanism is determined by the physical and chemical characteristic of the adsorbent as well as the mass adsorbent - adsorbate transfer process. As a result, the kinetic modelling data can be used to deduce the type of transport mechanism (Kołodyńska et al., 2018). Thus to establish an appropriate equation for characterizing the heavy metal ions adsorption process on ChBC and MBC, the kinetic data was fitted to the mathematical and nonlinear forms of PFO, PSO and Elovich models. Tables 1 and 2 present the calculated parameters of all kinetic models at the concentration 100 mg/dm^3.

Generally, the nonlinear regression of the Elovich equation presented the highest values of R^2 (>0.969) and the lowest values of χ^2 (<0.718) for Cd(II), Co(II) and Zn(II) ions sorption on both sorbents. Moreover, the applicability of the Elovich equation suggests that removal of these ions is of chemisorption character (Naima et al., 2022), (Wekoye et al., 2020). However, in the case of the PSO model, large values of the correlation coefficient (>0.917) and a smaller value of Chi-square (<2.222) were also obtained indicating that the equation can be applied for predicting adsorption of Cd(II), Co(II) and Zn(II) ions on ChBC and MBC. The PFO model shows the worst fit between the experimental and theoretical data.

On the other hand, in the case of Pb(II) ions the best fit (R^2=1.000) was exhibited by the PFO and PSO models with the smallest errors (< $9.440 \cdot 10^{-4}$). This is related to the immediate ion capture and the %S in 1 min. is 99.3%.

Table 1. Kinetic parameters of Cd(II), Co(II), Zn(II) and Pb(II) adsorption on ChBC

Model	Parameters	Heavy metal ions			
		Cd(II)	Co(II)	Zn(II)	Pb(II)
PFO	k_1 (1/min)	0.126	1.014	1.461	34255.991
	q_1 (mg/g)	15.27	10.30	16.69	17.39
	R^2	0.888	0.886	0.858	1.000
	χ^2	3.361	1.149	3.783	$2.520 \cdot 10^{-4}$
PSO	k_2 (g/mg·min)	0.011	0.134	0.112	20.09
	q_2 (mg/g)	16.34	10.76	17.39	17.40
	R^2	0.952	0.951	0.917	1.000
	χ^2	1.449	0.490	2.222	$3.40 \cdot 10^{-5}$
Elovich	α (mg/g·min)	16.20	19108.418	86678.793	$3.120 \cdot 10^{44}$
	β (g/mg)	0.439	1.362	0.895	6.279
	R^2	0.986	0.998	0.993	0.993
	χ^2	0.424	0.020	0.179	0.022

Table 2. Kinetic parameters of Cd(II), Co(II), Zn(II) and Pb(II) adsorption on MBC

Model	Parameters	Heavy metal ions			
		Cd(II)	Co(II)	Zn(II)	Pb(II)
PFO	k_1 (1/min)	1.017	0.555	0.352	36193.15
	q_1 (mg/g)	14.64	12.83	14.37	19.09
	R^2	0.932	0.825	0.906	1.000
	χ^2	1.329	2.960	1.978	$9.440 \cdot 10^{-4}$
PSO	k_2 (g/mg·min)	0.107	0.060	0.040	9.680
	q_2 (mg/g)	15.20	13.50	14.97	19.10
	R^2	0.980	0.922	0.967	1.000
	χ^2	0.387	1.326	0.709	$9.189 \cdot 10^{-6}$
Elovich	α (mg/g·min)	206637.93	825.70	499.35	$3.169 \cdot 10^{44}$
	β (g/mg)	1.113	0.826	0.716	5.712
	R^2	0.990	0.997	0.970	0.993
	χ^2	0.192	0.052	0.717	0.026

3.6. Sorption isotherm, temperature impact and thermodynamic tests

The sorption data provide the information on the adsorbent optimization and design as well as the explanation of the affinity and binding energy of the adsorbate - adsorbent. In addition, from the shape of the isotherm, there can be made a hypothesis about the adsorption method, i.e. whether it occurs on the monolayer or polylayer, whether the side interactions between the adsorbate molecules are involved and the nature of the adsorbent-adsorbate interactions (Hu et al., 2007). The Langmuir, Freundlich and Temkin isotherm models were used to present the equilibrium data of heavy metal ion sorption in this research (Fig. 7a). The adsorption parameters of these models were computed from the nonlinear

regression approach. In the order of the listed parameters (Tables 3 and 4), the experimental data gave the satisfactory fits: Freundlich > Temkin > Langmuir. The value of the correlation coefficient >0.960 determined from the Freundlich isotherm model is the highest suggesting a good fit to the experimental data. The Freundlich isotherm describes the sorption process on a multilayer heterogeneous adsorbent surface with different adsorption centres and on microporous adsorbents (Bazan-Wozniak & Pietrzak, 2019). Therefore it can to be expected that the process is reversible and not confined to the formation of a single adsorbent layer (Nanta et al., 2018), (Deng et al., 2021). The large value of R^2 calculated from the Temkin model shows that the electrostatic interactions play an important role in the sorption process (Aichour et al., 2022).

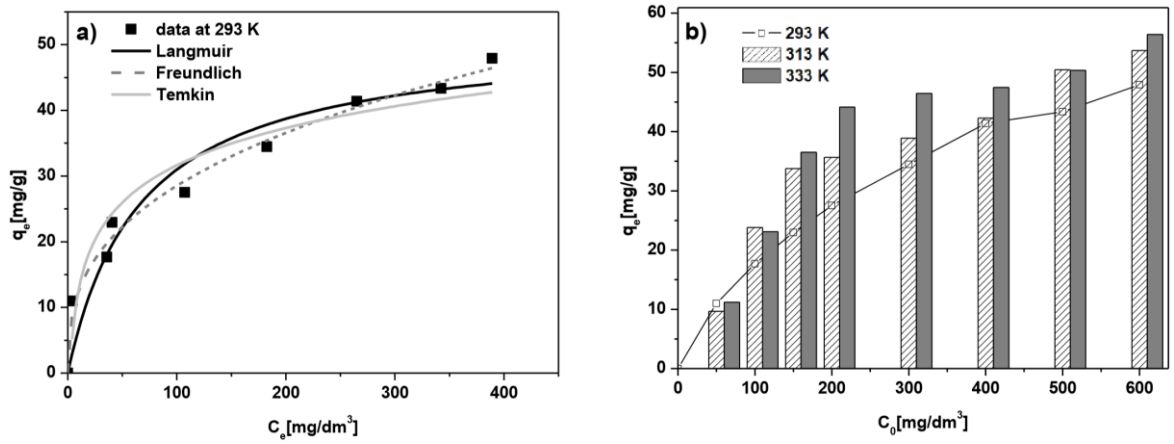

Fig. 7. (a) Nonlinear fit of the Langmuir, Freundlich and Temkin isotherm models, (b) impact of temperature on the Cd(II) sorption on ChBC (C_0 50-600 mg/dm^3, pH 5, shaking speed 180 rpm)

The sorption process of Cd(II) ions is temperature-dependent as shown by the data in Fig .7b and the q_e value grows with the increasing temperature, reaching the maximum at 333 K. The same results were obtained for the other ions (see in the Supplementary Materials - Fig. S3, S4, S5 and S6). It can be expected that with the increasing temperature, ions diffusion to the sorbent surface increases as well as the number of active centres rises which results in the reaction efficiency increase.

The thermodynamic parameters provide specific details regarding the energy changes during the adsorption. The positive values of ΔH^o suggested the endothermic process of heavy metal ions sorption on the biochar based sorbents. The decreasing negative values of $\Delta G°$ with the increasing temperature demonstrated that the sorption process is spontaneous and more effective at higher temperatures. In addition, the value in the range from -10.72 to -15.92 kJ/mol indicates the physical nature of Cd(II), Co(II), Zn(II), Pb(II) on ChBC and Cd(II), Co(II), Zn(II) on MBC sorption (-20 to 0 kJ/mol) (Konicki

Table 3. Isotherms modelling parameters of Cd(II), Co(II), Zn(II) and Pb(II) sorption on ChBC

Model	Parameters	Heavy metal ions			
		Cd(II)	Co(II)	Zn(II)	Pb(II)
Langmuir	q_m (mg/g)	51.63	79.91	42.711	59.704
	K_L (dm^3/mg)	0.015	0.003	0.065	0.047
	R^2	0.935	0.939	0.886	0.833
	χ^2	16.816	10.802	26.518	66.983
Freundlich	K_F (mg/g)	5.475	1.072	10.510	14.512
	n	2.790	1.617	3.862	3.955
	R^2	0.989	0.970	0.987	0.963
	χ^2	2.901	5.281	3.019	14.825
Temkin	A	0.478	0.146	4.048	45.664
	B	8.181	8.435	5.921	5.338
	R^2	0.935	0.829	0.956	0.865
	χ^2	16.778	30.336	10.105	54.091

Table 4. Isotherms modelling parameters of Cd(II), Co(II), Zn(II) and Pb(II) sorption on MBC

Model	Parameters	Heavy metal ions			
		Cd(II)	Co(II)	Zn(II)	Pb(II)
Langmuir	q_m (mg/g)	43.396	31.247	30.170	69.935
	K_L (dm³/mg)	0.042	0.026	0.258	4.122
	R^2	0.911	0.868	0.860	0.851
	χ^2	19.807	13.357	18.247	128.131
Freundlich	K_F (mg/g)	9.895	6.265	12.884	40.744
	n	3.903	3.803	5.967	3.722
	R^2	0.992	0.984	0.997	0.961
	χ^2	1.703	1.593	0.351	33.73
Temkin	A	8.663	3.302	92.849	230.170
	B	4.900	3.857	3.087	8.979
	R^2	0.929	0.925	0.975	0.890
	χ^2	15.773	7.623	3.311	94.229

Table 5. Thermodynamic parameters of Cd(II), Co(II), Zn(II) and Pb(II) sorption on ChBC and MBC.

Sorbent	Ions	K_d Temperature [K]			ΔH^o [kJ/mol]	ΔS^o [J/mol K]	E_a [kJ/mol]	ΔG^o [kJ/mol] Temperature [K]		
		293	313	333				293	313	333
ChBC	Cd(II)	121	141	154	4.55	55.58	37.08	-11.73	-12.85	-13.96
	Co(II)	112	128	170	6.97	63.26	17.32	-11.57	-12.83	-14.10
	Zn(II)	177	275	297	10.70	79.95	16.85	-12.73	-14.32	-15.92
	Pb(II)	275	311	322	3.25	57.88	15.93	-13.71	-14.87	-16.02
MBC	Cd(II)	126	130	130	0.70	42.61	17.58	-11.78	-12.64	-13.49
	Co(II)	81	108	134	10.21	71.42	19.37	-10.72	-12.14	-13.57
	Zn(II)	107	189	199	12.71	82.85	25.50	-11.57	-13.22	-14.88
	Pb(II)	8106	338766	519808	85.69	371.23	17.63	-23.08	-30.50	-37.93

et al., 2017). The values are from -23.08 to -37.93 kJ/mol, which corresponds to the processes of physic- and chemisorption - as is the case with the sorption of Pb(II) ions on MBC (in the range from -20 to -40 kJ/mol) (Demey et al., 2014). In adsorption research, activation energy is defined as the energy needed to react the adsorbate ions with the adsorbent. Physisorption processes typically need lower activation energies (0–4 kJ/mol), whereas chemisorption processes require higher activation energies (15–800 kJ/mol) due to the formation of stronger chemical interactions (Alaei et al., 2020). The research result obtained for the adsorption of M(II) ions on ChBC and MBC indicates that the adsorption process is a chemisorption.

Table 6 compares the maximum sorption capacities of the biochar based sorbents in the removal of heavy metal ions from the aqueous media applied. It can be stated that ChBC and MBC give satisfactory results for the Cd(II), Co(II), Zn(II) and Pb(II) ions capture. High sorption capacity of Pb(II) ions on nano-sized MgO particles modified biochar, biochar from wheat straw modified using $FeSO_4 \cdot 7H_2O$ and bone biochar modified by FeO_x particles, the modification process requires further optimization.

3.7. Regeneration of the biochar based sorbents

The economic effectiveness of adsorbent regeneration and future usage are determined by several factors. The analysis of the reversibility of the adsorption process of heavy metal ions on ChBC and MBC provides valuable information on the probable mechanism of the sorption process (Bassam et al., 2022). Furthermore, regeneration is necessary to restore the starting capacity of the adsorbent and to capture metal ions so that they can be appropriately disposed of to minimize further contamination (Igberase et al., 2019). After the sorption process, the dried and weighed sorbents were shaken with the

Table 6. Comparison of amounts of adsorbed heavy metal ions with various types of biochar modification

Ions	Sorbent	Adsorption capacity (mg/g)	References
Cd(II)	biochar from wheat straw modified using $FeSO_4 \cdot 7H_2O$	64.1	(Trakal et al., 2016)
	bone biochar modified by MnO_x particles	163.4	(Xiao et al., 2020)
	biochar thiolated using 3- mercaptopropyltrimethoxysilane	2.58	(Wang et al., 2021)
	biochar oxidized using H_2O_2	3.32	(Wang et al., 2021)
Co(II)	poly(acrylic acid) grafted chitosan and biochar composite	135.1	(Zhang et al., 2019)
Zn(II)	poly(acrylic acid) grafted chitosan and biochar composite	114.9	(Zhang et al., 2019)
	hydroxyapatite-biochar nanocomposite	47.5	(Wang et al., 2018)
	nano-sized MgO particles modified biochar	202.2	(Jellali et al., 2016)
Pb(II)	biochar from wheat straw modified using $FeSO_4 \cdot 7H_2O$	247.0	(Trakal et al., 2016)
	bone biochar modified by FeO_x particles	271.9	(Xiao et al., 2020)

acidic desorbing agents: HNO_3, HCl and H_2SO_4 at the concentration of 1 mol/dm^3 for 360 minutes. The results are given in Fig. 8. The desorption percentage values, confirm that HNO_3 leaches the heavy metal ions adsorbed on the ChBC and MBC most effectively. When comparing the desorption effectiveness of hydrochloric acid to that of sulfuric one, it can be concluded that HCl is characterized by larger desorption percentage values. For ChBC and MBC loaded Pb(II) applying sulfuric acid the smallest desorption percentage was equal to 14.8 and 12.2 %, respectively. This is a result of small solubility of lead sulfate confirming that this acid should not be used for the Pb(II) ions recovery. The most effective washing out of Pb(II) ions from ChBC with the desorption percentage 99.5 % was observed. In general, ChBC and MBC as heavy metal ions adsorbents are characterized by excellent regeneration and reuse capability.

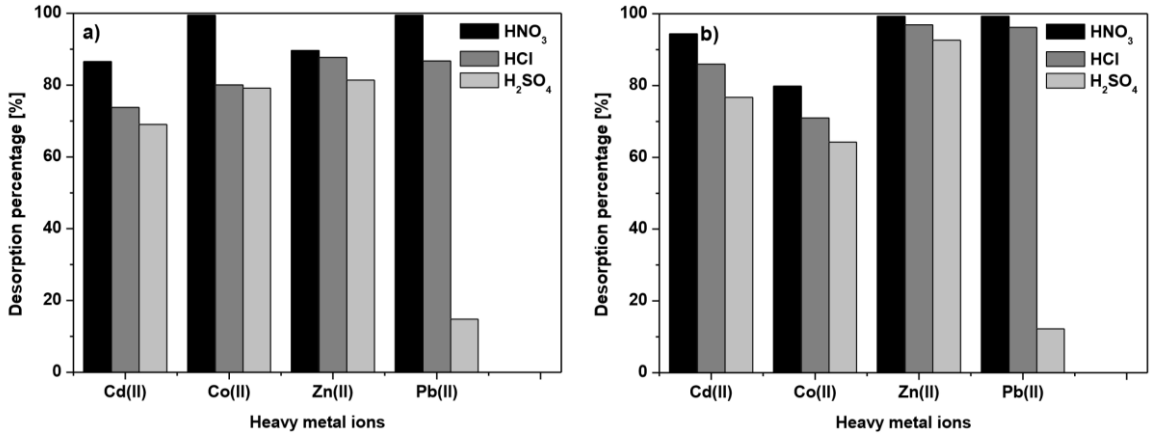

Fig. 8. Dependence of desorption percentage on M(II) ions sorption on (a) ChBC and (b) MBC using different acids in three sorption-desorption cycles

4. Conclusions

The biochar based sorbents ChBC and MBC were successfully developed and employed in the Cd(II), Co(II), Zn(II) and Pb(II) ions adsorption investigations with several advantages including effective removal capacity, low cost, easy processing and regeneration as well as reuse capability. The physicochemical methods confirmed the well-developed micro- and mesoporous structures containing the surface functional groups: carboxyl, hydroxyl and phenol on the modified biochars. The pH value 5 and the interaction time 360 minutes were found in the most effective sorption process. The Elovich

equation fitted the kinetics of Cd(II), Co(II) and Zn(II) ions data the best indicating that chemisorption is the rate limiting step. For Pb(II) ions, the best fit (R^2=1.000) and the smallest errors were obtained using the PFO and PSO models. The nonlinear form of the Freundlich model was efficient for description of the Cd(II), Co(II), Zn(II) and Pb(II) ions adsorption providing that the process is not confined to creating a single layer. The calculated Gibbs free energy values prove the physical nature of the adsorption of Cd(II), Co(II), Zn(II) and Pb(II) on ChBC and Cd(II), Co(II) and Zn(II) MBC and physi- and chemistorption of Pb(II) ions on MBC. But the activation energy calculations prove that the main adsorption mechanism is chemisorption. Both sorbents were regenerated the most effectively by the nitric acid solution. The research confirmed that the both biochar based sorbents had similar and great affinity for M(II) ions in the aqueous media which is satisfactory compared to the other biochar modifications described in the literature.

Acknowledgments

This research received no external funding.

References

AICHOUR, A., ZAGHOUANE-BOUDIAF, H., DJAFER KHODJA, H., 2022. *Highly removal of anionic dye from aqueous medium using a promising biochar derived from date palm petioles: Characterization, adsorption properties and reuse studies.* Arab. J. Chem. 15(1), 103542.

AKSU, Z., ISOGLU, I. A. 2005. *Removal of copper(II) ions from aqueous solution by biosorption onto agricultural waste sugar beet pulp.* Process Biochem. 40, 3031–3044.

ALAEI, R., JAVANSHIR, S., BEHNAMFARD, A., 2020. *Treatment of gold ore cyanidation wastewater by adsorption onto a Hydrotalcite-type anionic clay as a novel adsorbent.* J. Environ. Health Sci. Eng. 18(2), 779–791.

AMALINA, F., RAZAK, A. S. A., KRISHNAN, S., ZULARISAM, A. W., NASRULLAH, M., 2022. *A comprehensive assessment of the method for producing biochar, its characterization, stability, and potential applications in regenerative economic sustainability – A review.* Cleaner Mater. 3, 100045.

BAI, S., WANG, L., MA, F., ZHU, S., XIAO, T., YU, T., WANG, Y., 2020. *Self-assembly biochar colloids mycelial pellet for heavy metal removal from aqueous solution.* Chemosphere. 242, 125182.

BASSAM, R., EL ALOUANI, M., MAISSARA, J., JARMOUNI, N., BELHABRA, M., EL MAHI CHBIHI, M., BELAAOUAD, S., 2022. *Investigation of competitive adsorption and desorption of heavy metals from aqueous solution using raw rock: Characterization kinetic, isotherm, and thermodynamic.* Mater. Today: Proc. 52, 158–165.

BAZAN-WOZNIAK, A., PIETRZAK, R., 2019. *Activated bio-carbons prepared by physical activation of residues after supercritical extraction of raw plants.* Physicochem. Probl. Miner. Process. 55(6), 1357–1365.

BOZECKA, A., BOZECKI, P., SANAK-RYDLEWSKA, S., 2016. *Removal of Pb(II) and Cd(II) ions from aqueous.* Physicochem. Probl. Miner. Process. *52(1)*, 380–396.

CUI, X., DAI, X., KHAN, K. Y., LI, T., YANG, X., HE, Z., 2016. *Removal of phosphate from aqueous solution using magnesium-alginate/chitosan modified biochar microspheres derived from Thalia dealbata.* Bioresour. Technol. *218*, 1123–1132.

DAI, W., XU, M., ZHAO, Z., ZHENG, J., HUANG, F., WANG, H., LIU, C., XIAO, R., 2021. *Characteristics and quantification of mechanisms of Cd2+ adsorption by biochars derived from three different plant-based biomass.* Arab. J. Chem. 14(5), 103119.

DEMEY, H., VINCENT, T., RUIZ, M., SASTRE, A. M., GUIBAL, E., 2014. *Development of a new chitosan/Ni(OH)2 -based sorbent for boron removal.* Chem. Eng J. 244, 576–586.

DENG, X., CHI, R., XIAO, C., ZHANG, Z., LIU, X., HU, J., 2021. *The intensified effect of nitrogen removal properties using Pseudomonas fulva K3 and MgBC for the weathered crust rare earth wastewater treatment.* Physicochem. Probl. Miner. Process. 57(3), 69–84.

DUDEK, S., KOŁODYŃSKA, D., 2022. *Arsenate removal on the ion exchanger modified with cerium(III) ions.* Physicochem. Probl. Miner. Process. 58(2).

ELTAWEIL, A. S., OMER, A. M., EL-AQAPA, H. G., GABER, N. M., ATTIA, N. F., EL-SUBRUITI, G. M., MOHY-ELDIN, M. S., ABD EL-MONAEM, E. M., 2021. *Chitosan based adsorbents for the removal of phosphate and nitrate: A critical review.* Carbohydr. Polym. 274, 118671.

FARHANGI-ABRIZ, S., GHASSEMI-GOLEZANI, K., 2021. *Changes in soil properties and salt tolerance of safflower in response to biochar-based metal oxide nanocomposites of magnesium and manganese.* Ecotoxicol. Environ. Saf. 211,

111904.

GONG, H., CHI, J., DING, Z., ZHANG, F., HUANG, J., 2020. *Removal of lead from two polluted soils by magnetic wheat straw biochars.* Ecotoxicol. Environ. Saf. 205, 111132.

HAN, Z., SANI, B., MROZIK, W., OBST, M., BECKINGHAM, B., KARAPANAGIOTI, H. K., WERNER, D., 2015. *Magnetite impregnation effects on the sorbent properties of activated carbons and biochars.* Water Res. 70, 394–403.

HU, Q., XU, Z., QIAO, S., HAGHSERESHT, F., WILSON, M., LU, G. Q., 2007. *A novel color removal adsorbent from heterocoagulation of cationic and anionic clays*. J. Colloid Interface Sci. 308(1), 191–199.

HUANG, J., YUAN, F., ZENG, G., LI, X., GU, Y., SHI, L., LIU, W., SHI, Y., 2017. *Influence of pH on heavy metal speciation and removal from wastewater using micellar-enhanced ultrafiltration.* Chemosphere. 173, 199–206.

IGBERASE, E., OFOMAJA, A., OSIFO, P. O., 2019. Enhanced heavy metal ions adsorption by 4-aminobenzoic acid grafted on chitosan/epichlorohydrin composite: *Kinetics, isotherms, thermodynamics and desorption studies.* Int. J. Biol. Macromol. 123, 664–676.

JANU, R., MRLIK, V., RIBITSCH, D., HOFMAN, J., SEDLÁČEK, P., BIELSKÁ, L., SOJA, G., 2021. *Biochar surface functional groups as affected by biomass feedstock, biochar composition and pyrolysis temperature.* Carbon Resour. Convers. 4, 36–46.

JELLALI, S., DIAMANTOPOULOS, E., HADDAD, K., ANANE, M., DURNER, W., MLAYAH, A., 2016. *Lead removal from aqueous solutions by raw sawdust and magnesium pretreated biochar: Experimental investigations and numerical modelling.* J. Environ. Manage. 180, 439–449.

KOŁODYŃSKA, D., BĄK, J., KOZIOŁ, M., PYLYPCHUK, L. V., 2017. *Investigations of Heavy Metal Ion Sorption Using Nanocomposites of Iron-Modified Biochar.* Nanoscale Res. Lett. 12.

KOŁODYŃSKA, D., KRUKOWSKA, J., THOMAS, P., 2017. *Comparison of sorption and desorption studies of heavy metal ions from biochar and commercial active carbon.* Chem. Eng. J. 307, 353–363.

KOŁODYŃSKA, DOROTA, BĄK, J., MAJDAŃSKA, M., FILA, D., 2018. *Sorption of lanthanide ions on biochar composites.* J. Rare Earths. 36(11), 1212–1220.

KONICKI, W., ALEKSANDRZAK, M., MIJOWSKA, E., 2017. *Equilibrium, kinetic and thermodynamic studies on adsorption of cationic dyes from aqueous solutions using graphene oxide.* Chem. Eng. Res. Des. 123, 35–49.

LEE, H. S., SHIN, H. S. (2021). *Competitive adsorption of heavy metals onto modified biochars: Comparison of biochar properties and modification methods.* J. Environ. Manage.299, 113651.

LI, B., JING, F., HU, Z., LIU, Y., XIAO, B., GUO, D., 2021. *Simultaneous recovery of nitrogen and phosphorus from biogas slurry by Fe-modified biochar.* J. Saudi Chem. Soc. 25(4), 101213.

NAIMA, A., AMMAR, F., ABDELKADER, O., RACHID, C., LYNDA, H., SYAFIUDDIN, A., BOOPATHY, R., 2022. *Development of a novel and efficient biochar produced from pepper stem for effective ibuprofen removal*. Bioresour. Technol. 347, 126685.

NANTA, P., KASEMWONG, K., SKOLPAP, W., 2018. *Isotherm and kinetic modeling on superparamagnetic nanoparticles adsorption of polysaccharide.* J. Environ.Chem.Eng. 6(1), 794–802.

OTREMBSKA, P., GEGA, J., 2013. *Kinetic studies on Sorption of Ni(II) and Cd(II) from chloride solutions using selected acidic cation exchangers.* Physicochem. Probl. Miner. Process. 49(1), 301–312.

QAMBRANI, N. A., RAHMAN, M. M., WON, S., SHIM, S., RA, C., 2017. *Biochar properties and eco-friendly applications for climate change mitigation, waste management, and wastewater treatment : A review.* Renew. Sust. Energ. Rev. 79, 255–273.

QU, J., DONG, M., WEI, S., MENG, Q., HU, L., HU, Q., WANG, L., HAN, W., ZHANG, Y., 2020. *Microwave-assisted one pot synthesis of β-cyclodextrin modified biochar for concurrent removal of Pb(II) and bisphenol a in water*. Carbohydr. Polym. 250.

RAJAPAKSHA, A. U., CHEN, S. S., TSANG, D. C. W., ZHANG, M., VITHANAGE, M., MANDAL, S., GAO, B., BOLAN, N. S., OK, Y. S., 2016. *Engineered/designer biochar for contaminant removal/immobilization from soil and water: Potential and implication of biochar modification.* Chemosphere. 148, 276–291.

RAMA CHANDRAIAH, M., 2016. *Facile synthesis of zero valent iron magnetic biochar composites for Pb(II) removal from the aqueous medium.* Alex. Eng. J. 55(1), 619–625.

RANGABHASHIYAM, S., LINS, P. V. DO. S., OLIVEIRA, L. M. T. D. M., SEPULVEDA, P., IGHALO, J. O., RAJAPAKSHA, A. U., MEILI, L., 2022. *Sewage sludge-derived biochar for the adsorptive removal of wastewater pollutants:* A critical review. Environ. Pollut. 293(November 2021).

SBIZZARO, M., CÉSAR SAMPAIO, S., RINALDO DOS REIS, R., DE ASSIS BERALDI, F., MEDINA ROSA, D., MARIA BRANCO DE FREITAS MAIA, C., SARAMAGO DE CARVALHO MARQUES DOS SANTOS

CORDOVIL, C., TILLVITZ DO NASCIMENTO, C., ANTONIO DA SILVA, E., EDUARDO BORBA, C., 2021. *Effect of production temperature in biochar properties from bamboo culm and its influences on atrazine adsorption from aqueous systems.* J. Mol. Liq. 343, 117667.

SHARAF EL-DEEN, S. E. A., MOUSSA, S. I., MEKAWY, Z. A., SHEHATA, M. K. K., SADEEK, S. A., SOMEDA, H. H., 2017. *Evaluation of CNTs/MnO2 composite for adsorption of 60Co(II), 65Zn(II) and Cd(II) ions from aqueous solutions.* Radiochim. Acta. 105(1), 43–55.

SOČO, E., KALEMBKIEWICZ, J., 2015. *Removal of copper(II) and zinc(II) ions from aqueous solution by chemical treatment of coal fly ash.* Croat. Chem. Acta. 88(3), 267–279.

TAN, Y., WAN, X., NI, X., WANG, L., ZHOU, T., SUN, H., WANG, N., YIN, X., 2022. *Efficient removal of Cd(II) from aqueous solution by chitosan modified kiwi branch biochar.* Chemosphere. 289(Ii).

TAN, Z., LIN, C. S. K., JI, X., RAINEY, T. J., 2017. *Returning biochar to fields: A review.* Appl. Soil Ecol. 116, 1–11.

TRAKAL, L., VESELSKÁ, V., ŠAFARIK, I., VÍTKOVÁ, M., CˇÍHALOVÁ, S., KOMÁREK, M., 2016. *Lead and cadmium sorption mechanisms on magnetically modified biochars.* Bioresour. Technol. 203, 318–324.

WANG, C., WANG, H., *2018. Pb(II) sorption from aqueous solution by novel biochar loaded with nano-particles.* Chemosphere. 192, 1–4.

WANG, F., JIN, L., GUO, C., MIN, L., ZHANG, P., SUN, H., ZHU, H., ZHANG, C., 2021. *Enhanced heavy metals sorption by modified biochars derived from pig manure.* Sci. Total Environ. 786, 147595.

WANG, Y., LIU, Y., LU, H., YANG, R., YANG, S., 2018. *Competitive adsorption of Pb(II), Cu(II) and Zn(II) ions onto hydroxyapatite-biochar nanocomposite in aqueous solutions*. J. Solid State Chem. 261, 53–61.

WEKOYE, J. N., WANYONYI, W. C., WANGILA, P. T., TONUI, M. K., 2020. *Kinetic and equilibrium studies of Congo red dye adsorption on cabbage waste powder.* Environ. Chem. Ecotoxicol. 2, 24–31.

XIAO, J., HU, R., GUANGCAI, C., XING, B., 2020. *Facile synthesis of multifunctional bone biochar composites decorated with Fe/Mn oxide micro-nanoparticles: Physicochemical properties, heavy metals sorption behavior and mechanism*. J. Hazard. Mater. 399, 123067.

XIE, J., LIN, R., LIANG, Z., ZHAO, Z., YANG, C., CUI, F., 2021. *Effect of cations on the enhanced adsorption of cationic dye in Fe3O4-loaded biochar and mechanism.* J. Environ. Chem. Eng. 9(4), 105744.

ZHANG, L., TANG, S., HE, F., LIU, Y., MAO, W., GUAN, Y., 2019. *Highly efficient and selective capture of heavy metals by poly(acrylic acid) grafted chitosan and biochar composite for wastewater treatment.* Chem. Eng. J. 378, 122215.

ZHANG, W., TAN, X., GU, Y., LIU, S., LIU, Y., HU, X., LI, J., ZHOU, Y., LIU, S., HE, Y., 2020. *Rice waste biochars produced at different pyrolysis temperatures for arsenic and cadmium abatement and detoxification in sediment*. Chemosphere. 250, 126268.

ZHOU, Y., BIN GAO, A. R. Z., FANG, J., YINING SUN, CAO, X., 2013. *Sorption of heavy metals on chitosan-modified biochars and its biological effects.* Chem. Eng. J. 231, 512–518.